Distributed Range-Free Localization of Wireless Sensor Networks via Nonlinear Dynamics

Shuai Li and Yangming Li

Additional information is available at the end of the chapter

http://dx.doi.org/10.5772/49093

1. Introduction

In the past years, the development in micro electromechanical systems (MEMS), radio frequency (RF), integrated circuit (IC), etc., greatly enhanced the advancement of wireless sensor networks (WSNs). As an ubiquitous sensing technology, WSNs find more and more applications, such as structural monitoring [34], precision agriculture [3], gas-leak localization [14], volcano monitoring [33], robot navigation [4, 15], health monitoring [20], to name a few. For most existing applications of WSNs, the location information is crucial. For example, in the structural monitoring application, we can conclude that the structure is out of condition if fault is detected by one or more sensors in the network of sensors mounted everywhere on the structure. However, we are unable to accurately report the faulty position without localization capability of the WSN. In contrast to other type of networks, e.g., Internet, a prominent difference is that WSNs are location-based networks. Therefore, the design of localization hardware and localization algorithms is an important procedure in the development of a WSN system.

There are mainly two classes of localization approaches for WSNs: one is pre-localization and the other one is self-localization. The pre-localization method measures the position of sensors in the deployment stage. After the deployment and position measurement, the position is stored in the memory of the sensor. For this method, any movement of the sensors will result in errors in the location information. Differently, the self-localization method computes the locations of each sensor based on real-time measurements and therefore is robust to the variance of the environment. With GPS devices embedded, sensors are enabled with self-localization capability. However, the relatively high cost of GPS devices often makes it not practical to apply GPS to all sensors in a network. Instead, the strategy with a portion of sensors equipped with GPS as beacons and using triangulation or trilateration to iteratively determine the positions of blind sensors based on the distance or angle measurements between neighboring sensors provides a less expensive way for self-localization [13, 16, 26]. Although many GPS devices are saved, as a tradeoff, the sensors are required to have the ability to measure the distance or the relative angle to its neighbor, which may result in

costs for extra hardware. Without introducing extra hardware, received signal strength (RSS) based distance measurement method [17, 30], relying on the estimated distance according to the signal strength received from the neighboring sensor, provides a promising direction for self-localization. Another promising self-localization method is range-free localization, which even does not require the information on the signal strength received from the neighbor but the connectivity information, i.e., a sensor only need to know who is its neighbor. This technology implies that localization can be a by-product of communication since connectivity information can be obtained in communication. For example, if Sensor A can communicate with Sensor B, then we conclude they are connected. Due to this promising property, range-free localization is becoming more and more popular in both practice and research. In this chapter, we investigate the range-free localization of WSNs.

Dynamic models gained great success in realtime signal processing [28], robotics [12, 22], online optimization [29], etc.. In this chapter, we overview our previous work on dynamic model based range-free localization [10, 11, 25]. Particularly, we will examine two dynamic models for the real time localization of WSNs. The models are described by nonlinear ordinary differential equations (ODEs). The state value of the ODEs converges to the expected position estimation of sensors. Both of the two models find feasible solutions to the formulated optimization problem. Particularly, the second model, by exploiting heuristic information, has a tendency to converge to better solutions in the sense of localization error. The real time processing ability of the models allows possible movement of the sensor nodes, which often happens in mobile sensor networks [23]. Besides the real time localization capability, another prominent feature of the proposed models is that both of them are completely distributed, i.e., each sensor in the network only need to exchange information with its neighbor and thus no message passing is needed in the network. This advantage makes the proposed algorithms scalable to large scale networks involving thousands of sensors or more.

The remainder of this paper is organized as follows. In Section 2, some preliminaries on range-free localization of WSNs are presented. In Section 3, we formulate the localization problem from an optimization perspective. Two dynamic models are presented in Section 4 to solve the formulated optimization problems. In Section 5, simulations are performed to demonstrate the effectiveness of our method. Section 6 concludes this paper.

2. Preliminaries

In this chapter, we assume that all sensors are equipped with communication modules and the locations of beacon sensors are known. Fig. 1 sketches the connectivity topology of a WSN consisting of beacon sensors and blind sensors. In the network, The beacon sensors are those with known locations. The locations can be obtained either by GPS or by pre-deployment. The blind sensors are those without pre-known positions. A sensor can communicate with other sensors within the signal coverage area. The communication links and sensors therefore form a network with sensors as nodes and communication links as edges.

The signal strength at a given distance from the emitter varies due to propagation conditions, material coverage, antenna configurations and battery conditions [31] and the calculated distance according to the received signal strength often has a large error [8, 18]. Nevertheless, the nominal maximum range, which is measured under ideal conditions in open environments without obstacles along the signal propagation route, without material coverage, with a proper configuration of the antenna and with a full power of the battery, etc.,
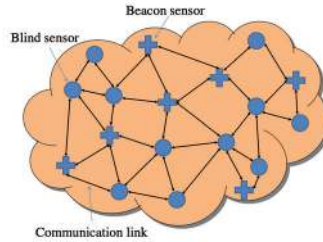
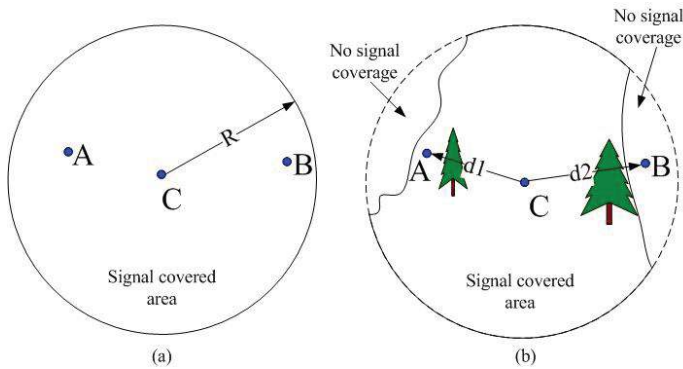**Figure 1.** Schematic of a WSN topology in two dimensional space.

Figure 2. Range-free localization in environments with obstacles.

gives an upper bound on the distance between the emitter and receiver pair. As depicted in Fig. 2. Subfigure (a) depicts the ideal open environment, where the communication radius, denoted by R in the figure, equals the nominal maximum range. In this situation, both the point A and the point B are within the communication range of the sensor located at point C and therefore the distance from the sensor to A and that to B are both less than R. In the situation with the presence of obstacles (shown as trees in the subfigure (b)), the signal covered area shrinks and some positions, such as the point B in the subfigure (b), even with a distance less than R to the sensor, cannot be covered by the signal. Therefore, $d1$, which is the distance from the sensor to point A, is less than R if the sensor located at A can detect the signal.

3. Problem formulation

In this section, we present the mathematical formulation of the problem.

3.1. Nonlinear inequality problem formulation

As discussed in Section 2, the position of beacon sensors are known and the distance between two neighbor sensor (in the sense of communication) is less than R, which is the nominal

maximum communication range. In equation, we have

$$(x_i - x_j)^T(x_i - x_j) \leq R^2 \quad \text{for } i \in \mathbb{N}(j) \tag{1a}$$

$$x_k = \bar{x}_k \quad \text{for } k \in \mathbb{B} \tag{1b}$$

where $\mathbb{B}$ is the beacon sensor set, x_i, x_j represent the position of the ith sensor and the jth sensor, respectively, R is the maximum communication range of sensors, $\mathbb{N}(j)$ denotes the jth sensor's neighbor set, which includes all sensors connected to it via communication, $\mathbb{B}$ is the beacon sensor set, $\bar{x}_k$ is the true position of the kth beacon sensor.

Remark 1. *There is no explicit objective function but inequality and equality constraints in problem (1). The solution to this problem is generally not unique. We are more concerned with finding a feasible solution in real time instead of finding all the feasible solutions. Based on this consideration, we explore finding a feasible solution to problem (1) in real time via a dynamic model.*

3.2. Optimization problem formulation

To find a feasible solution of problem (1) numerically, we first transform the problem into an optimization problem and employ dynamic evolutions to solve it.

The solution of problem (1) is identical to the one of the following normal optimization with an explicit objective function,

$$\text{minimize} \quad \sum_{i=1}^{n} \sum_{j \in \mathbb{N}(i)} w_{ij} \max\{(x_i - x_j)^T(x_i - x_j) - R^2, 0\}$$

$$\text{subject to} \quad x_k = \bar{x}_k \quad \text{for } k \in \mathbb{B} \tag{2}$$

where n denotes the number of sensors, $w_{ij} > 0$ is the weight of the connection between the ith and the jth sensor. Note that the problem (2) is a non-smooth optimization problem due to the presence of the function $\max(\cdot)$.

4. Solving the problem via nonlinear dynamic evolution

In this section, we present two ODE models, both of which are able to solve the range-free localization problem (2). As the solution to the problem is generally not unique. Property employment of heuristic information may improve the solution performance. Based on the feasible solution obtained by the first ODE model, the second ODE model proposed in this chapter indeed realizes the improvement in performance.

4.1. Model I

The partial sub-gradient relative to x_i of the objective function switches between $4\sum_{j \in \mathbb{N}(i)}(x_i - x_j)$ and 0 at the critical point $(x_i - x_j)^T(x_i - x_j) - R^2 = 0$. For smooth arbitration, we use the following dynamic evolution to find a feasible solution of the optimization problem (2),

$$\dot{x}_i = -\epsilon_1 \sum_{j \in \mathbb{N}(i)} w_{ij} I_{ij}(x_i - x_j) \tag{3}$$

where x_i is the position estimation of the blind sensor labeled i, which is initialized randomly, $\epsilon_1 > 0$ is a scaling factor, w_{ij} is a positive weight, I_{ij} is an indicator function defined as follows:

$$I_{ij} = \begin{cases} 1 & \text{if } (x_i - x_j)^T (x_i - x_j) - R^2 > 0 \\ 0 & \text{if } (x_i - x_j)^T (x_i - x_j) - R^2 \leq 0 \end{cases} \tag{4}$$

In the ODE model, each blind sensor is associated with a dynamic module. The modules interact with their neighbor modules and all the modules together perform the localization task and solve the problem (1). The dynamic evolution of x_i in the system (3) depends on its neighbor values x_j for $j \in \mathbb{N}(i)$. In detail, the neighbor x_j has an action $-\epsilon_1 I_{ij}(x_i - x_j)$ on x_i. This action term is analogous to a force pointing from x_i to x_j and pulling x_i to x_j with an amplitude ϵ_1 or 0 respectively when $\|x_i - x_j\| > R$ or $\|x_i - x_j\| \leq R$. This negative feedback mechanism guides position estimations of neighbor sensors to aggregate to within the maximum range R.

Notably, the ODE model (3) is a distributed one. Communication only happens between neighboring sensors. No routing or cross-hop communication is required for the implementation of the ODE model. The distributed nature of the model thoroughly reduces the communication burden and makes the method scalable to a network with a large number of sensors involved.

About the ODE model I (3), we have the following theorem,

Theorem 1 ([25]). *The ODE model I (3) with $\epsilon_1 > 0$, w_{ij} for all possible i and j, asymptotically converges to a feasible solution x_i^* (for all i in the blind sensor set) of problem (1).*

The proof of this theorem is based on Lyapunov stability theory. Interested readers are refereed to our previous work [10, 25] for a detailed proof. This theorem reveals that the ultimate output of the ODE model I is a feasible solution to problem (1).

4.2. Model II

Section 4.1 provides an ODE model to find a feasible solution of the problem. The model presented in this part is also a dynamic ODE model. Different from Model I, which is initialized randomly and does not use any heuristic information, Model II is initialized with the ultimate output of Model I with R replaced by $R - \delta$ in (4) with $\delta \ll R$ and takes advantages of heuristic information to result in sensor position estimations with inclination to uniformly distribution. We first define the following optimization problem to incorporate heuristic information,

$$\text{minimize} \quad \sum_{i=1}^{n} \sum_{j \in \mathbb{N}(i)} (x_i - x_j)^T (x_i - x_j)$$

$$- c_0 \sum_{i=1}^{n} \sum_{j \in \mathbb{N}(i)} \log \left(R^2 - (x_i - x_j)^T (x_i - x_j) \right) \tag{5a}$$

$$x_k = \bar{x}_k \quad \text{for } k \in \mathbb{B} \tag{5b}$$

where $\mathbb{B}$ is the beacon sensor set, x_i is initialized with the ultimate output of (3) with R replaced by $R - \delta$ in (4). $c_0 > 0$ is a coefficient. Note that the first term in (5a) contributes to the

equal distribution in space. In (5a) the terms involving x_i write $2\sum_{j\in\mathbb{N}(i)}(x_i - x_j)^T(x_i - x_j)$. The minimization of $2\sum_{j\in\mathbb{N}(i)}(x_i - x_j)^T(x_i - x_j)$ in terms of x_i tends to adapt x_i to the center formed by all x_j for $j \in \mathbb{N}(i)$. The second term in (5a) is essentially a barrier term and approaches to infinitely large when the solution tends to violate the inequality constraints given in (1). This term works to restrict the solution in the feasible set.

We use the following gradient based dynamics to solve (5):

$$\dot{x}_i = -\epsilon_2 \sum_{j\in\mathbb{N}(i)} \left(1 + \frac{c_0}{R^2 - (x_i - x_j)^T(x_i - x_j)}\right)(x_i - x_j)$$
$$x_k = \bar{x}_k \quad \text{for } k \in \mathbb{B}$$
$$x_i(0) = x_i' \tag{6}$$

where x_i is the position estimation of the ith blind sensor, x_i' is the ultimate output of Model I (3) with R replaced by $R - \delta$, i.e., the solution of x_i obtained by solving (2) with R replaced by $R - \delta$ in (4). The expression $x_i(0) = x_i'$ means that x_i is initialized with x_i'. $\epsilon_2 > 0$ is a scaling factor and $c_0 > 0$ is a positive constant.

The ODE model (6) is a distributed one since the update of x_i in (6) only depends on x_j for $j \in \mathbb{N}(i)$, i.e., the position estimations of the neighbor sensors. Therefore, communication only happens between neighbor sensors.

About the initialization of the ODE model, we have the following remark,

Remark 2. *The ODE model (6) is initialized with the ultimate output of the ODE model I (3) with R replaced by $R - \delta$ in (4) with $\delta \ll R$. The goal is to ensure the ultimate output of Model I strictly locates inside the open set formed by (1), which is necessary for the barrier term in (5) to restrict the solution always stays inside the feasible region.*

According to Theorem 1, the ODE model I with R replaced by $R - \delta$ ultimately converges to a solution in the following set,

$$(x_i - x_j)^T(x_i - x_j) \leq (R - \delta)^2 \quad \text{for } i \in \mathbb{N}(j) \tag{7a}$$
$$x_k = \bar{x}_k \quad \text{for } k \in \mathbb{B} \tag{7b}$$

with which we conclude that $(x_i - x_j)^T(x_i - x_j) \leq (R - \delta)^2 < R^2$ for $i \in \mathbb{N}(j)$. With the effect of the barrier term $\frac{c_0}{R^2 - (x_i - x_j)^T(x_i - x_j)}(x_i - x_j)$ in the model II (6), the ultimate solution of (6) with an initialization inside the feasible set will still stay inside this set. We have the following theorem to state this point rigourously,

Theorem 2 ([11]). *The ODE model II (6) with $\epsilon_2 > 0$, $c_0 > 0$, initialized with x_i', which is the ultimate output of the ODE model I (3) with R replaced by $R - \delta$ in (4) with $\delta \ll R$, stays in the open set constructed by (1).*

5. Simulations

In this section, simulations are used to verify the two ODE models in both the one dimensional space and the two dimensional space.
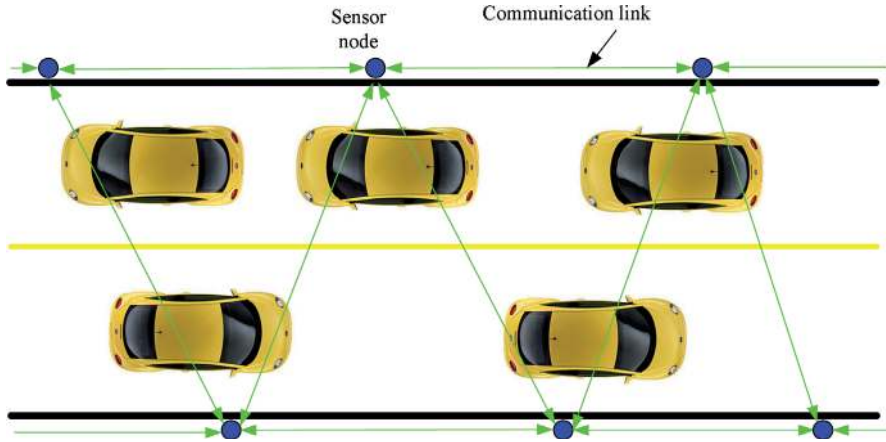
Figure 3. A schematic description of WSNs for highway monitoring.

5.1. Range-free localization in one dimensional spaces

In this part, we investigate the range-free localization of sensors in a network deployed in a one dimensional topology.

5.1.1. Background

There are a bunch of applications which deploys sensors along an one dimensional line. For example, WSNs for highway monitoring [1, 9, 21] are often deployed along the highway direction and thus form a one dimensional deployment topology, as sketched in Fig. 3. Other applications, such as WSNs for bridge health monitoring [32] and WSNs along a tunnel [5] for traffic safety, can also be put into the category of one dimensional localization problem.

5.1.2. Simulation setup and simulation results

We consider a wireless sensor network with one dimensional deployment. There are 4 beacon sensors deployed at 0m, 166.6667m, 333.3333m and 500.0000m, and 16 blind sensors deployed at 26.6011m, 56.1963m, 83.3216, 119.9182m, 147.7692m, 176.9903m, 208.3049m, 238.5405m, 263.6398m, 290.4771m, 320.4868m, 355.1442m, 384.0493m, 407.3632m, 440.0192m and 470.5006m, respectively. The communication range of sensors is 50m.

For the dynamic models, the state values of Model I are randomly initialized. We choose $\epsilon_1 = 10^5$, $\epsilon_2 = 20 \times 10^5$ as the scaling parameters, the coefficient $c_0 = 5$. The shrinking constant δ is chosen as 5. Fig. 4 plots the transient behavior of the position estimation by Model I. From this figure, we can clearly see that the estimation converges with time. For Model II, it is initialized with the output of Model I by replacing R with $R - \delta$. As $R \approx R - \delta$ in this simulation, Fig. 4 and Fig. 5, which shows the transient to obtain the initial position estimation for Model II, demonstrate similar behaviors. Fig. 6 shows the transient of the position estimation by Model II. By comparing the final values and the initial values in Fig. 6, it can be found that the values tends to equal distances between neighbors. The position estimation results are shown in Fig. 7. It can be observed that both models result in estimations meeting the nonlinear inequalities (neighbor sensors are within a distance of 50m). However, the result by Model I may break
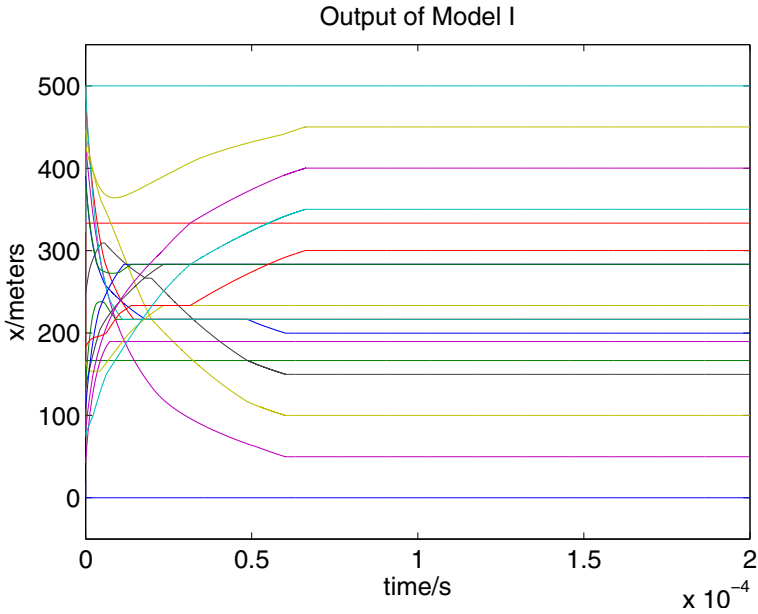
Output of Model I

Figure 4. Transient of the position estimation by Model I in the one dimensional localization problem.

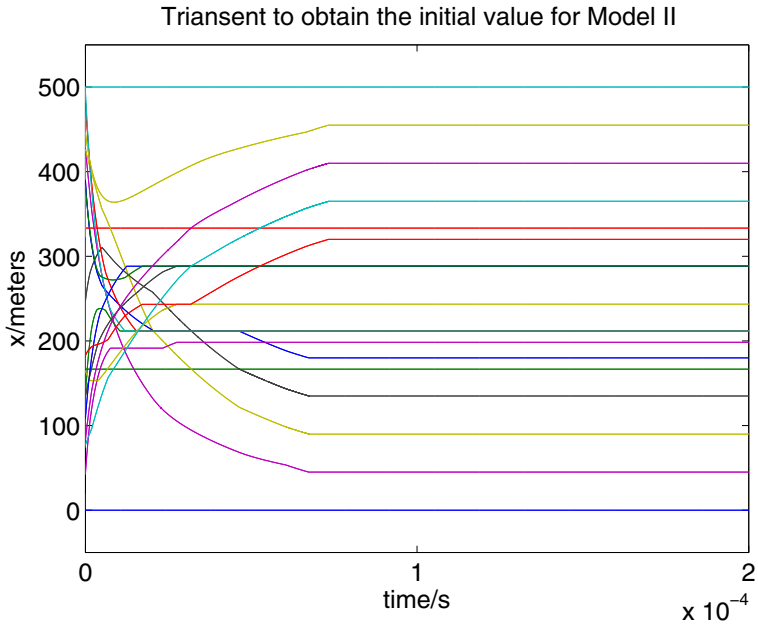Triansent to obtain the initial value for Model II

Figure 5. Transient to obtain the initial position estimation for Model II in the one dimensional localization problem.

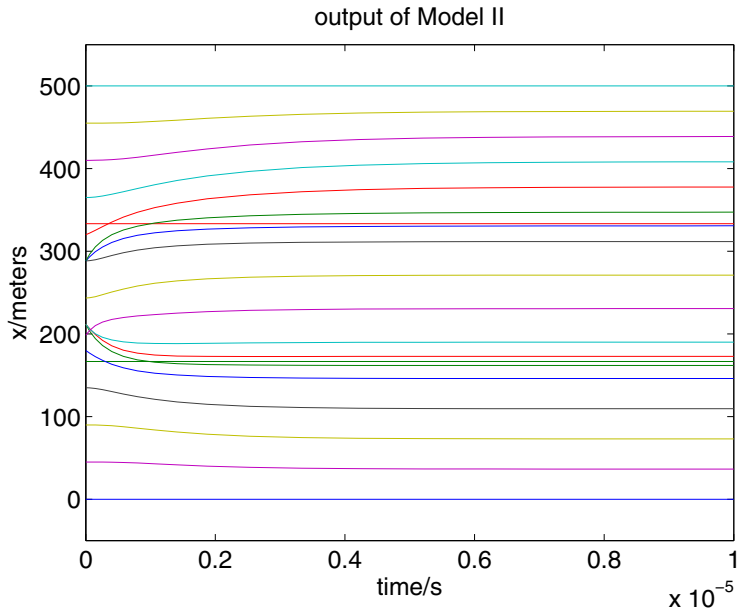**Figure 6.** Transient of the position estimation by Model II in the one dimensional localization problem.
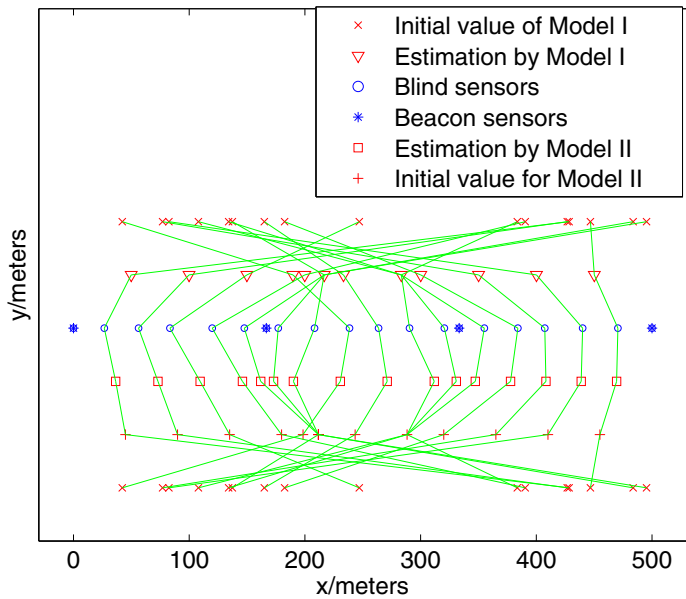

Figure 7. Position estimation results in the one dimensional localization problem.

the real order, i.e., as shown in Fig. 7 the sixth sensor from the left actually locates to the left of the eighth one while the estimated position of the sixth sensor by Model I is to the right of the eighth sensor. However, the performance is improved by using Model II and the estimation results follows the real order. For better comparisons of Model I and Model II in the sense of estimation error, we use the Root-mean-square error $E1$ defined as $E1 = \sqrt{\frac{\sum_{i=1}^{n} ||\hat{x}_i - x_i||^2}{n}}$ (where $\hat{x}_i$ and x_i represent the estimated value and the true value of the ith sensor's position), and the maximum absolute error $E2$ defined as $E2 = \max_{i=1,2,...,n}\{||\hat{x}_i - x_i||\}$ to evaluate the estimation error. Ten independent simulations with random initializations are performed and the estimation errors are calculated for all runs. As shown in Table 1, the error $E1$ is around 40 and the error $E2$ is around 80 for Model I with the simulation setup. In contrast, the estimation errors for Model II are much lower, which are about 10 for $E1$ and 26 for $E2$ in the ten simulation runs. This result demonstrates the advantage of Model II over Model I for position estimation of sensors by introducing heuristic information. Also note that there are only 4 beacon sensors in contrast to 16 blind sensors, meaning that the ratio of beacon sensors to blind sensors is 25%. For such a low beacon vs. blind sensor ratio, the estimation errors $E1$ and $E2$ for both Model I and Model II, especially for Model II, as shown in Table 1, are acceptable for rough estimations of sensor positions in applications.

♯	Estimation Error of Model I		Estimation Error of Model II	
	E1	E2	E1	E2
1	41.2948	84.0870	9.9419	23.7890
2	44.5053	84.4876	10.2123	27.2300
3	43.7765	80.0258	13.2497	26.1105
4	44.3971	83.3457	11.1692	26.9130
5	40.9815	83.3549	12.4231	28.3951
6	40.7992	79.4815	10.8819	25.6199
7	39.5168	86.9493	11.4397	26.0199
8	37.4373	65.4550	10.4166	24.0404
9	42.9898	83.3865	11.4330	26.6570
10	44.0201	78.4496	13.2752	28.7782

Table 1. Estimation errors for Model I and Model II in different simulation runs of the one dimensional localization problem.

5.2. Range-free localization in two dimensional Spaces

In this part, we investigate the range-free localization of sensors in a network deployed in a two dimensional topology.

5.2.1. Background

Most existing literatures deal with the general localization problem in two dimensional space. The one dimensional sensor localization problem investigated in the last section falls into this category by fixing the value of sensor positions along one dimension. Localization in applications, such as wildlife monitoring [7], WSN aided robot navigation [6, 19] and animal tracking [27], can be abstracted as two dimensional localization problems.

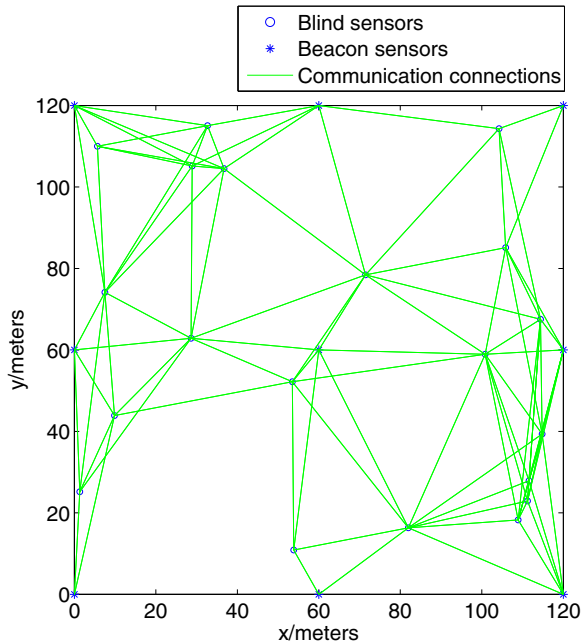*5.2.2. Simulation setup and simulation results*

Figure 8. True positions of sensors in a typical simulation run of the two dimensional WSN localization problem.

In the simulation, we consider a $100 \times 100 m^2$ square area with 9 beacon sensors uniformly deployed (the beacon sensors are deployed along the perimeter and at the center, with relative coordinates $[0, 0]$m, $[60, 0]$m, $[120, 0]$m, $[0, 60]$, $[60, 60]$, $[120, 60]$, $[0, 120]$, $[60, 120]$, $[120, 120]$ respectively.) and 20 blind sensors randomly deployed (see Fig. 8 for the deployment of sensors in a typical simulation run). The maximum communication range of sensors are chosen as $R = 50$m.

As to the dynamic models, we choose the scaling factors $\epsilon_1 = \epsilon_2 = 10^5$, the connection weight w_{ij} equals 5 for connections with a beacon sensor and 1 otherwise for Model I, the relaxation parameter $delta = 0.5$ for Model II and the coefficient $c_0 = 1$ for Model II.

Fig. 9 and Fig. 10 show the time histories of the position estimations by Model I along x-direction and that along y-direction respectively. From the figures we can observe that after a short period of transient, the estimation results converge to constant values. The time histories of the position estimations along x-direction and y-direction estimations by Model II are plotted in Fig. 11 and Fig. 12, respectively. Compared to the transient of Model I, the change of state values in Fig. 11 and Fig. 12 are much milder. The adjustment of values refine the initial estimation with the tendency to even distributions under the communication connectivity constraints. With time elapses, the estimation results by Model II converge. It is worth noting that the ultimate values by Model II shown in Fig 11 and Fig. 12 are not exactly uniformly distributed. This is due to the compromise of the heuristic information driving to even
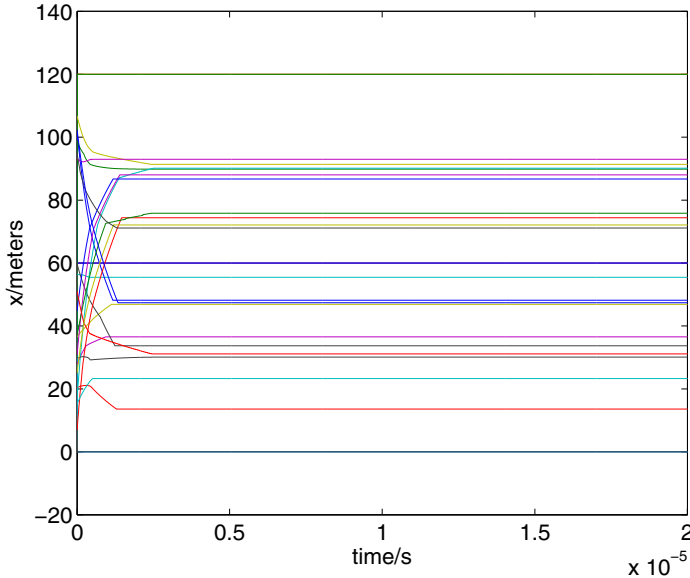
Figure 9. Time history of the position estimation in x-direction by Model I in the two dimensional WSN localization problem.

distribution in space and the inequality constraints imposed by communication connectivity. The final position estimations by Model I and Model II are shown in Fig. 13 and Fig. 14, respectively. It can be observed that the estimated results shown in both figures are within the area covered by the circle centered at the true position with a radius $R = 50$m, which verifies the effectiveness of Model I and Model II in modeling the communication connectivity constraint. On the other hand, it is clear that the estimation results shown in Fig. 14 outperforms the results shown in Fig. 13 thank to introducing heuristic information in Model II. For better comparisons of Model I and Model II for estimating sensor locations in two dimensional scenario, the Root-mean-square error $E1$ defined as $E1 = \sqrt{\frac{\sum_{i=1}^{n} ||\hat{x}_i - x_i||^2}{n}}$ and the maximum absolute error $E2$ defined as $E2 = \max_{i=1,2,...,n}\{||\hat{x}_i - x_i||\}$, both of which are the same as the definition in the one dimensional case, are used to evaluate the estimation error. Ten independent simulations with random initializations are performed and the estimation errors are calculated for all runs. As shown in Table 2, the error $E1$ is around 20 and the error $E2$ is around $r0$ for Model I with the simulation setup. In contrast, the estimation errors for Model II are about 10 for $E1$ and 20 for $E2$ in the ten simulation runs, which are much lower than the results obtained by Model I and again verifies the advantage of Model II in position estimation.

5.3. Discussions

In the above two subsections, we considered the range-free localization problem in one dimensional case and two dimensional case respectively. In some applications of WSNs, higher dimensional cases [24] (see Fig. 15 for the sketch of a typical three dimensional one
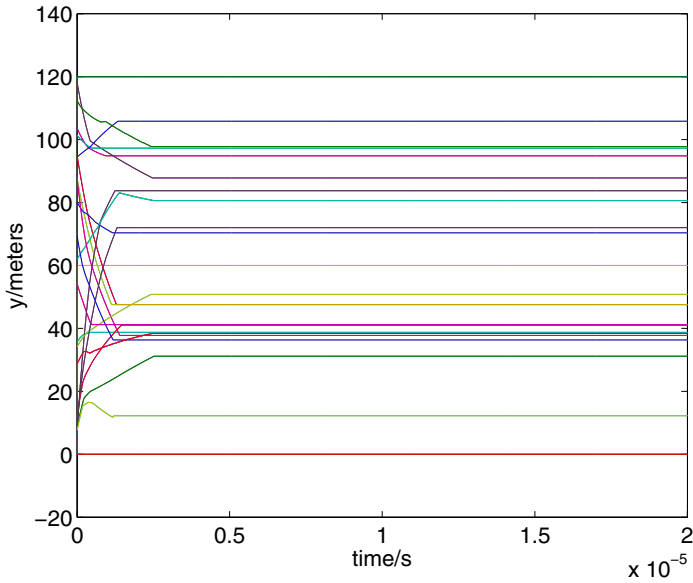
Figure 10. Time history of the position estimation in y-direction by Model I in the two dimensional WSN localization problem.

♯	Estimation Error of Model I		Estimation Error of Model II	
	E1	E2	E1	E2
1	19.2071	34.9071	10.9093	24.0850
2	20.6657	42.7582	10.2647	18.3666
3	21.2873	37.9441	10.2106	18.2110
4	20.0403	41.3617	9.9603	16.8761
5	20.6692	39.0069	9.1838	17.2634
6	18.1865	40.7181	9.5004	21.8774
7	21.0053	37.7784	10.2448	18.6334
8	23.1289	44.2787	12.3591	25.5854
9	23.5922	40.3665	10.6922	21.0049
10	19.5115	41.8718	11.6586	24.0909

Table 2. Estimation errors for Model I and Model II in different simulation runs of the one dimensional localization problem.
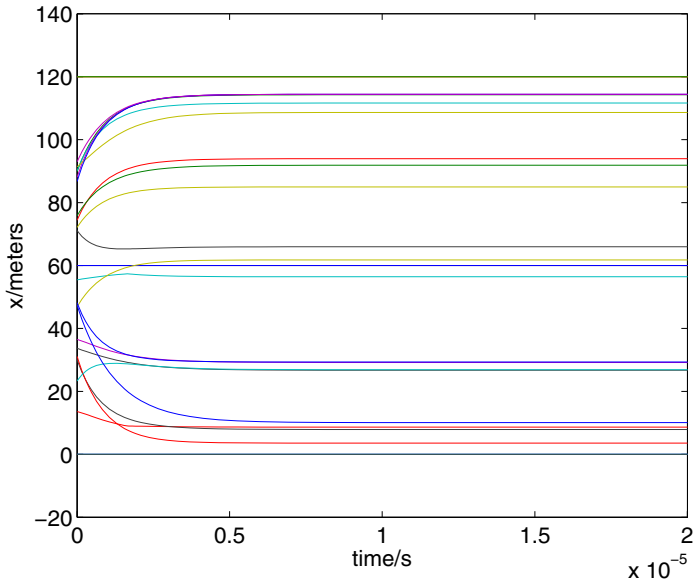
Figure 11. Time history of the position estimation in x-direction by Model II in the two dimensional WSN localization problem.
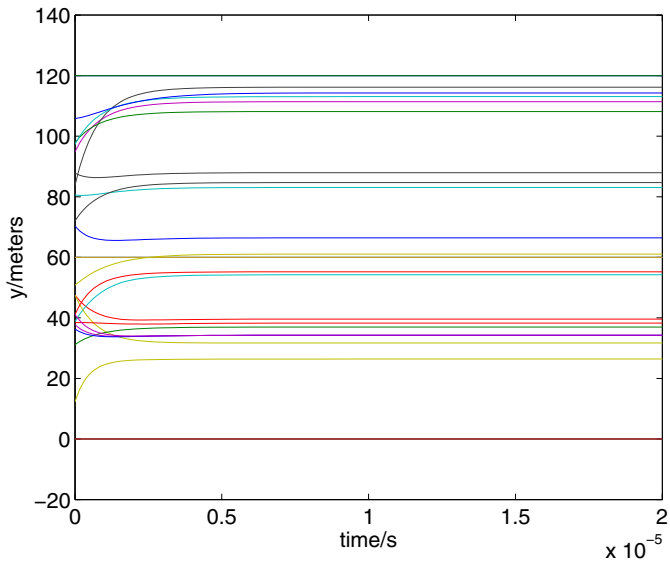

Figure 12. Time history of the position estimation in y-direction by Model II in the two dimensional WSN localization problem.
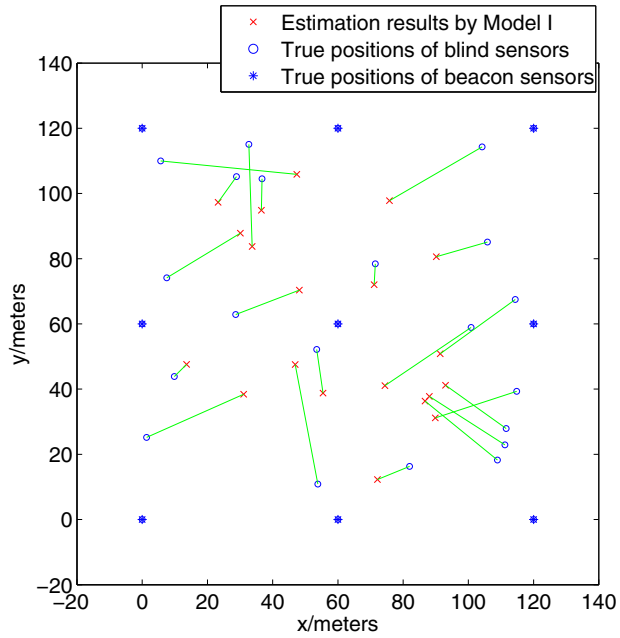
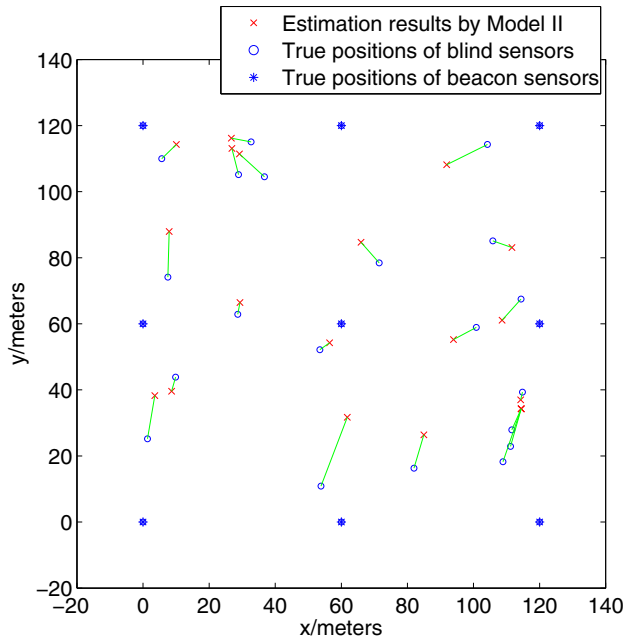**Figure 13.** Position estimation results by Model I in the two dimensional WSN localization problem.

Figure 14. Position estimation results by Model II in the two dimensional WSN localization problem.

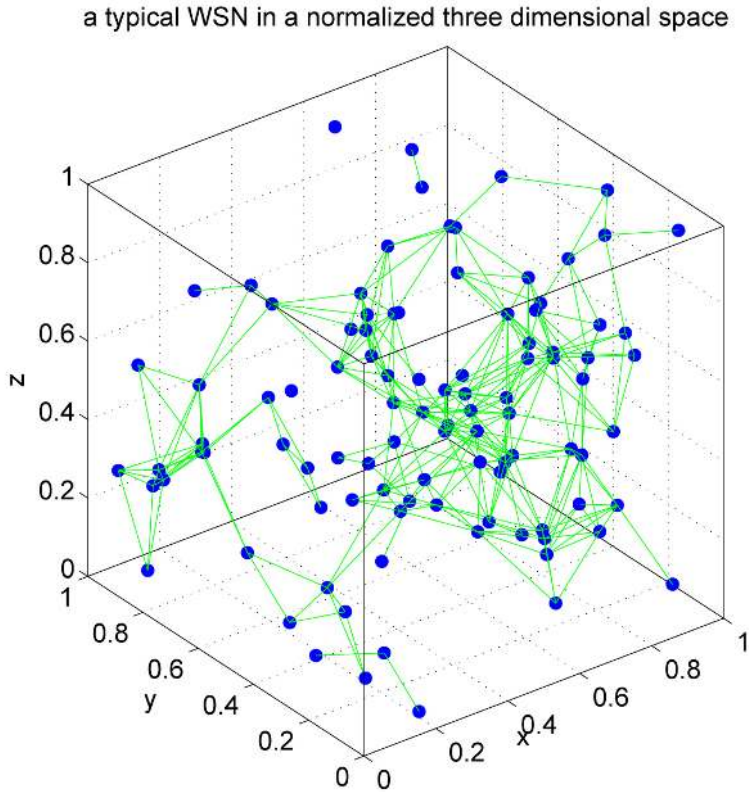a typical WSN in a normalized three dimensional space

Figure 15. A typical WSN in normalized three dimensional space.

after normalization along three axial directions), such as building monitoring [35], underwater acoustic sensor networks[2], may be encountered. For example, the localization problem of sensors for building monitoring is actually defined in a three dimensional space since sensors are deployed in two dimensions on each floor and the whole network constructed by sensors on different floors forms a three dimensional one. Also, sensors in the underwater acoustic sensor networks are often deployed at different depth, with different longitude and latitude and thus form a three dimensional sensor network.

The presented two models in this chapter admit the higher dimensional localization problems as we did not specify the number of dimensions in the problem formulation and the model works for all possible dimensions.

As demonstrated in simulations, Model II outperforms Model I in the sense of estimation error for the cases with the same simulation setup. However, it is notable that Model II requires an extra dynamic model for the initialization, which is at the cost of implementation complexity and longer computation time. Fortunately, the dynamic models can be implemented with either digital or analog devices and thus the computation can be completed in a very short time. For example, the simulation examples for the two dimensional localization problem

showed that it takes a time of 10^{-5} level for the dynamic models to converge. As to the implementation complexity, more hardware devices, such as summators, multipliers, dividers, integrators, etc, are needed to fabricate the analog circuit of Model II than that of Model I.

6. Conclusions and future work

In this chapter, we overviewed our recent work on range-free localization of sensors in WSNs via dynamic models. The range-free localization problem is formulated as two different optimization problems, each of which corresponds to a dynamic model, namely Model I and Model II, for the solution. Simulations in both one dimensional case and two dimensional case are performed and the two models are compared in both sceneries. The simulation results demonstrate effectiveness of the dynamic models.

Compared with conventional range-free localization algorithms, a prominent advantage of ODE based solutions is that the models are implementable by parallel hardware. As a promising direction for WSN localization, the following aspects are of fundamentally importance in both theory and practise and are open to all researchers,

• Is there better heuristic information applicable to improve the performance?

• Can Model II be modeled from a probabilistic perspective and therefore to evaluate its performance improvement relative to Model I in quantity?

• Recent advancement in ODE shows that a properly designed ODE model can receive finite time convergence to its steady state value. Can the results applied to the range-free WSN localization to gain a theoretically finite time convergence?

• Hardware implementation with VLSI, FPGA, etc. is a bright direction in practise.

• Can the presented models be used in range-base WSN localization, if not applicable directly, is the results helpful to supply a good "warm start", which accelerates the convergence?

• The presented models are essentially ODE models for solving nonlinear inequalities defined on a network. Are the models extendable to other network applications, such as robotic networks, smart grids, the internet of things, etc?

Acknowledgements

Author details

Shuai Li
Stevens Institute of Technology, USA

Yangming Li
Robot Sensor and Human-machine Interaction Lab, Institute of Intelligent Machines, Chinese Academy of Sciences, China

7. References

[1] Aalamifar, F., Vijay, G., Abedi Khoozani, P. & Ibnkahla, M. [2011]. Cognitive wireless sensor networks for highway safety, *Proceedings of the first ACM international symposium on Design and analysis of intelligent vehicular networks and applications*, DIVANet '11, ACM, New York, NY, USA, pp. 55–60.

[2] Akyildiz, I. F., Pompili, D. & Melodia, T. [2005]. Underwater acoustic sensor networks: Research challenges, *AD HOC NETWORKS (ELSEVIER* **3**: 257–279.

[3] Baggio, A. [2005]. Wireless sensor networks in precision agriculture, *Precision Agriculture* pp. 1–22.

[4] Batalin, M., Sukhatme, G. & Hattig, M. [2004]. Mobile robot navigation using a sensor network, *Robotics and Automation, 2004. Proceedings. ICRA '04. 2004 IEEE International Conference on*, Vol. 1, pp. 636 – 641 Vol.1.

[5] Ceriotti, M., Corra, M., D'Orazio, L., Doriguzzi, R., Facchin, D., Guna, S., Jesi, G., Cigno, R., Mottola, L., Murphy, A., Pescalli, M., Picco, G., Pregnolato, D. & Torghele, C. [2011]. Is there light at the ends of the tunnel? wireless sensor networks for adaptive lighting in road tunnels, *Information Processing in Sensor Networks (IPSN), 2011 10th International Conference on*, pp. 187 –198.

[6] Chen, W., Liang, H., Mei, T., You, Z., Miao, S., Li, S., Zhou, Y. & Meng, M. Q.-H. [2007]. Design and implementation of wireless sensor network for robot navigation., *I. J. Information Acquisition* pp. 77–89.

[7] Hu, W., Bulusu, N., Chou, C. T., Jha, S., Taylor, A. & Tran, V. N. [2009]. Design and evaluation of a hybrid sensor network for cane toad monitoring, *ACM Trans. Sen. Netw.* **5**(1): 4:1–4:28.

[8] Kaemarungsi, K. & Krishnamurthy, P. [2004]. Properties of indoor received signal strength for wlan location fingerprinting, *Mobile and Ubiquitous Systems: Networking and Services, 2004. MOBIQUITOUS 2004. The First Annual International Conference on*, pp. 14 – 23.

[9] Khanafer, M., Guennoun, M. & Mouftah, H. T. [2009]. Wsn architectures for intelligent transportation systems, *Proceedings of the 3rd international conference on New technologies, mobility and security*, NTMS'09, IEEE Press, Piscataway, NJ, USA, pp. 425–432.

[10] Li, S., Chen, S., Lou, Y., Lu, B. & Liang, Y. [2012]. A recurrent neural network for inter-localization of mobile phones, *IJCNN 2012*.

[11] Li, S., Liu, B., Chen, B. & Lou, Y. [2012]. Neural network based mobile phone localization using bluetooth connectivity, *NEURAL COMPUTING & APPLICATIONS* (0): –.

[12] Li, S., Meng, M. & Chen, W. [2007a]. Sp-nn: A novel neural network approach for path planning, *Robotics and Biomimetics, 2007. IEEE International Conference on*, pp. 1355 –1360.

[13] Li, S., Meng, M. & Liang, H. [2007]. A localization error estimation method based on maximum likelihood for wireless sensor networks, *Mechatronics and Automation, 2007. ICMA 2007. International Conference on*, pp. 348 –353.

[14] Li, S., Zhang, Z. & Ma, Y. [2007]. A sensor networks based method for detecting mine methane, *Information Acquisition, 2007. ICIA '07. International Conference on*, pp. 403 –407.

[15] Li, Y. [2010]. *Research On Robust Mapping Methods In Unstructured Environments*, PhD thesis, University of Science and Technology of China.

[16] Li, Y., Meng, M. & Chen, W. [2007b]. Data fusion based on rbf and nonparametric estimation for localization in wireless sensor networks, *Robotics and Biomimetics, 2007. ROBIO 2007. IEEE International Conference on*, pp. 1361 –1365.

[17] Li, Y., Meng, M., Li, S., Chen, W. & Liang, H. [2008]. Particle filtering for range-based localization in wireless sensor networks, *Intelligent Control and Automation, 2008. WCICA 2008. 7th World Congress on*, pp. 1629 –1634.

[18] Li, Y., Meng, M., Liang, H., Li, S. & Chen, W. [2008a]. Particle filtering for wsn aided slam, *Advanced Intelligent Mechatronics, 2008. AIM 2008. IEEE/ASME International Conference on*, IEEE, pp. 740–745.

[19] Li, Y., Meng, M. Q.-H., Liang, H., Li, S. & Chen, W. [2008b]. On wsn-aided simultaneous localization and mapping based on particle filtering, *Robot* **30**(5): 421–427.

[20] Milenkovi, A., Otto, C. & Jovanov, E. [2006]. Wireless sensor networks for personal health monitoring: Issues and an implementation, *Computer Communications (Special issue: Wireless Sensor Networks: Performance, Reliability, Security, and Beyond* **29**: 2521–2533.

[21] Mouftah, H. T., Khanafer, M., Guennoun, M. & Ave, K. E. [n.d.]. Wireless sensor network architectures for intelligent vehicular systems, pp. 1–7.

[22] Ogata, T., Nishide, S., Kozima, H., Komatani, K. & Okuno, H. [2010]. Inter-modality mapping in robot with recurrent neural network, *Pattern Recognition Letters* **31**(12): 1560–1569.

[23] Ogren, P., Fiorelli, E. & Leonard, N. [2004]. Cooperative control of mobile sensor networks:adaptive gradient climbing in a distributed environment, *Automatic Control, IEEE Transactions on* **49**(8): 1292 – 1302.

[24] Ortiz, C., Puig, J., Palau, C. & Esteve, M. [2007]. 3d wireless sensor network modeling and simulation, *Sensor Technologies and Applications, 2007. SensorComm 2007. International Conference on*, pp. 307 –312.

[25] S. Li, Y. L. & Liu, B. [2012]. Bluetooth aided mobile phone localization: a nonlinear neural circuit approach., *ACM Transactions on Embedded Computing Systems* **17**.

[26] Savvides, A., Srivastava, M., Girod, L. & Estrin, D. [2004]. Wireless sensor networks, Kluwer Academic Publishers, Norwell, MA, USA, chapter Localization in sensor networks, pp. 327–349.

[27] Sikka, P., Corke, P. I. & Overs, L. [2004]. Wireless sensor devices for animal tracking and control., *LCN'04*, pp. 446–454.

[28] Skowronski, M. & Harris, J. [2007]. Noise-robust automatic speech recognition using a predictive echo state network, *IEEE Transactions On Audio Speech And Language Processing* **15**(5): 1724–1730.

[29] Smith, K. [1999]. Neural networks for combinatorial optimization: a review of more than a decade of research, *INFORMS J. on Computing* **11**: 15–34.

[30] Taraktas, K., Ceylan, O. & Yagci, B. [2010]. Received signal strength technique performance in sensor network localization application, *Broadband, Wireless Computing, Communication and Applications (BWCCA), 2010 International Conference on*, pp. 357 –362.

[31] Tse, D. & Viswanath, P. [2005]. *Fundamentals of wireless communication*, Cambridge University Press, New York, NY, USA.

[32] VanZwol, T. R., Cheng, J. J. R. & Tadros, G. [2008]. Structural health monitoring of the golden gate bridge, *Canadian Journal of Civil Engineering* **35**(2): 179–189.

[33] Werner-Allen, G., Lorincz, K., Ruiz, M., Marcillo, O., Johnson, J., Lees, J. & Welsh, M. [2006]. Deploying a wireless sensor network on an active volcano, *Internet Computing, IEEE* **10**(2): 18 – 25.

[34] Xu, N., Rangwala, S., Chintalapudi, K. K., Ganesan, D., Broad, A., Govindan, R. & Estrin, D. [2004]. A wireless sensor network for structural monitoring, *Proceedings of the 2nd*

international conference on Embedded networked sensor systems, SenSys '04, ACM, New York, NY, USA, pp. 13–24.

[35] Zhou, J., Chen, Y., Leong, B. & Sundaramoorthy, P. S. [2010]. Practical 3d geographic routing for wireless sensor networks, *Proceedings of the 8th ACM Conference on Embedded Networked Sensor Systems*, SenSys '10, ACM, New York, NY, USA, pp. 337–350.